DOI: 10.1534/genetics.106.062604

Functional Analysis of Maize RAD51 in Meiosis and Double-Strand Break Repair

Jin Li,*,†,[1] Lisa C. Harper,‡ Inna Golubovskaya,‡ C. Rachel Wang,‡ David Weber,§ Robert B. Meeley, John McElver,**,[2] Ben Bowen,**,[3] W. Zacheus Cande‡ and Patrick S. Schnable*,†,††,‡‡,[4]**

**Department of Genetics, Development and Cell Biology, Iowa State University, Ames, Iowa 50011, †Interdepartmental Genetics Program, Iowa State University, Ames, Iowa 50011, ‡Department of Molecular and Cell Biology, University of California, Berkeley, California, 94720-3200, §Department of Biological Sciences, Illinois State University, Normal, Illinois 61790, **Pioneer Hi-Bred, Johnston, Iowa 50131, ††Department of Agronomy, Iowa State University, Ames, Iowa 50011 and ‡‡Center for Plant Genomics, Iowa State Unversity, Ames, Iowa 50011*

Manuscript received June 29, 2006
Accepted for publication May 8, 2007

ABSTRACT

In *Saccharomyces cerevisiae*, Rad51p plays a central role in homologous recombination and the repair of double-strand breaks (DSBs). Double mutants of the two *Zea mays* L. (maize) *rad51* homologs are viable and develop well under normal conditions, but are male sterile and have substantially reduced seed set. Light microscopic analyses of male meiosis in these plants reveal reduced homologous pairing, synapsis of nonhomologous chromosomes, reduced bivalents at diakinesis, numerous chromosome breaks at anaphase I, and that >33% of quartets carry cells that either lack an organized nucleolus or have two nucleoli. This indicates that RAD51 is required for efficient chromosome pairing and its absence results in nonhomologous pairing and synapsis. These phenotypes differ from those of an Arabidopsis *rad51* mutant that exhibits completely disrupted chromosome pairing and synapsis during meiosis. Unexpectedly, surviving female gametes produced by maize *rad51* double mutants are euploid and exhibit near-normal rates of meiotic crossovers. The finding that maize *rad51* double mutant embryos are extremely susceptible to radiation-induced DSBs demonstrates a conserved role for RAD51 in the repair of mitotic DSBs in plants, vertebrates, and yeast.

MEMBERS of the RecA-like protein family are required for homologous recombination and DNA repair (Roca and Cox 1990). Rad51p, a *recA* homolog of yeast, polymerizes *in vitro* on double-strand DNA to form a helical filament that is nearly identical, at least at low resolution, to the three-dimensional (3-D) structure formed by RecA (Ogawa *et al.* 1993). Rad51p can also bind single-stranded DNA and mediate DNA strand exchange *in vitro* (Sung 1994; Benson *et al.* 1998; New *et al.* 1998; Shinohara and Ogawa 1998). *In vivo* Rad51p forms complexes with Rad52p, Rad55p, Rad57p, and Dmc1p (Bishop 1994; Hays *et al.* 1995). When cultured in sporulation medium, yeast *rad51* mutant diploid cells can produce 10–20% spores relative to wild type, implying defects in meiosis. Rarely formed asci contain dyads and triads; very few contain tetrads (Shinohara *et al.* 1992). On the basis of mutant analysis, it appears that Rad51p and Dmc1p have overlapping functions in meiotic crossovers. Rates of meiotic crossovers decrease substantially as compared to wild type only when both proteins are eliminated (Shinohara *et al.* 1997; Grishchuk and Kohli 2003).

RAD51 homologs have been cloned from several plant species (Terasawa *et al.* 1995; Doutriaux *et al.* 1998; Franklin *et al.* 1999). Maize has two closely related genes, *Zmrad51a* and *Zmrad51b* (Franklin *et al.* 1999), which encode RecA-related proteins (Figure 1). To be consistent with nomenclature in other organisms, *Zmrad51a* and *Zmrad51b* are hereby renamed *Zmrad51A1* and *Zmrad51A2*, respectively. (In this article these two genes will be referred to as *rad51A1* and *rad51A2* except in those instances where the *Zm* prefix is required for clarity.) It has been suggested that in addition to its role in mediating DNA transfer, the maize RAD51 protein may be involved in homology search during meiosis (Franklin *et al.* 1999; Pawlowski *et al.* 2003).

A reverse genetic approach was used to functionally characterize the two maize *rad51* genes. Analysis of *rad51A1*

Sequence data from this article have been deposited with the EMBL/GenBank Data Libraries under accession no. AY359681.

[1]*Present address:* Department of Biology and Rosenstiel Center, Brandeis University, Waltham, MA 02254.

[2]*Present address:* BASF Plant Science, L.L.C, Research Triangle Park, NC 27709.

[3]*Present address:* Gene-*fx*, Berkeley, CA 94705.

[4]*Corresponding author:* Roy J. Carver Co-Lab Iowa State University Ames, IA 50011-3650. E-mail: schnable@iastate.edu

and *rad51A2* single and double mutants established that although *rad51A1* and *rad51A2* have at least partially redundant functions, RAD51 function is required for efficient chromosome pairing, homologous synapsis, proper chromosome segregation, and double-strand break (DSB) repair in meiosis. Although maize plants that lack RAD51 function survive and even flower, dry kernels of *rad51* double mutants are highly sensitive to radiation treatment. *rad51* double mutants are male sterile and exhibit a greatly reduced production of viable female gametes. Surprisingly, the rate of meiotic crossovers in these surviving female gametes does not differ significantly from that of wild type.

MATERIALS AND METHODS

Genetic stocks and crosses: The female parent of cross 1 is a *Mu* stock derived from those of Robertson (1978, 1980, 1981) via crosses to the hybrid B77 × B79 and Q66 × Q67. The inbred line B73 is fixed for functional alleles of *rad51A1* (*Rad51A1-B73*) and *rad51A2* (*Rad51A2-B73*); mutant alleles were maintained via crosses to B73. A material transfer agreement governs the distribution of the trait utility system for corn (TUSC) *Mu* insertion alleles of *rad51A1* and *rad51A2*; inquiries should be directed to R. B. Meeley.

Cross 1: *Mu Rad51A2/Rad51A2* × *rad51A2-98E7/Rad51A2*.
Cross 2: *Mu rad51A2-98E7/Rad51A2* × B73.

Characterization of *Mu* transposons and insertion sites in *rad51* TUSC alleles: Members of the *Mu* transposon family share ~200 bp conserved terminal repeats (TIRs). PCR was performed on each TUSC *Mu*-insertion allele using a series of gene-specific primers in combination with a primer (Mu-TIR) located in the highly conserved *Mu* TIRs. The resulting PCR products were purified and sequenced. These PCR products contain *Mu* TIR sequences terminal to the Mu-TIR primer annealing site. Comparing the TIR sequences from each of the *Mu*-insertion alleles to the left and right TIRs of each of the previously defined classes of *Mu* transposons established which class of *Mu* transposon was responsible for each TUSC allele. The resulting PCR products also contained *rad51* sequences between the positions of the *Mu* insertion site and the *rad51*-specific primer. Comparison of these PCR sequences to the *rad51* genomic sequences established the position of the *Mu* insertion in each TUSC allele.

Screen for deletion derivatives of *rad51A2-98E7*: Approximately 1000 kernels were planted in a 96-well format and tissues from up to four seedlings were bulked for DNA extraction (Dietrich *et al.* 2002) in the initial screen. Individual seedlings from a pool that contained a deletion candidate were transplanted to large pots for further growth. Leaf samples from each plant were recollected and DNA isolated. The PCR screen was repeated to identify the individual plant that carried a putative deletion derivative.

The PCR screen was performed using the Mu-TIR primer in conjunction with the *rad51A2*-specific primer 13219. In the absence of a structural rearrangement at the *rad51A2* locus, this primer pair will produce a 395-bp PCR product. In contrast, PCR amplification of DNA from a plant that carries a deletion of DNA between the annealing sites of primers 13219 and Mu-TIR would be expected to yield a smaller product.

The PCR products derived from deletion candidates were purified using the Qiaquick gel extraction kit (QIAGEN) and sequenced using the Mu-TIR primer. As a control, PCR products from *rad51A2-98E7* were purified and sequenced at the same time.

Molecular characterization of derivative alleles: Any of three possible types of sequence rearrangements can generate derivative alleles from *rad51A2-98E7* that yield smaller PCR products when amplifying with a *rad51A2*-specific primer 13219 in combination with a Mu-TIR primer: an intragenic *Mu* transposition, an insertion of an additional *Mu* transposon, or a deletion of *rad51A2* sequences adjacent to the original *Mu* insertion. To differentiate an intragenic transposition from an adjacent deletion, a second PCR reaction was performed using the Mu-TIR primer in combination with a *rad51A2*-specific primer RB-98E7 whose binding site is on the opposite side of the *Mu* insertion as compared to the primer 13219 used in the initial screen. If a derivative allele arose via an adjacent deletion, the PCR product from the other side should be the same size between *rad51A2-98E7* and the derivative allele. In contrast, if an allele arose via an intragenic transposition, the PCR product from the other side of the *Mu* insertion would be larger than the PCR product obtained from *rad51A2-98E7*. To differentiate between the insertion of an additional *Mu* transposon and an adjacent deletion, a primer rbdel was designed to anneal to the region thought to have been deleted. If a derivative allele arose via an adjacent deletion, this primer pair would not be expected to yield a PCR product. In contrast, if a derivative allele arose via the insertion of a second *Mu* transposon, amplification with Mu-TIR and rbdel would be expected to yield a *rad51A2*-specific PCR product.

Deletion derivative of *rad51A1-54F11*: While genotyping a family segregating for *rad51A1-54F11* using primer pair Mu-TIR and 11981, one plant (00-2608-1) with a smaller-size PCR product was identified. PCR-based experiments similar to those conducted on *rad51A2-98E7* derivatives established that this allele (designated *rad51A1-54F11d1*) is a deletion derivative of *rad51A1-54F11* (Figures 2 and 3).

Genotyping: The primer pair Mu-TIR and 11981 amplify *Mu* insertion alleles *rad51A1-54F11* and *rad51A1-54F11d1*. Because the wild-type *Rad51A1* allele in our stock is from inbred line B73, one indel polymorphism (IDP) marker (raidp31) can anneal to *Rad51A1-B73* but not to *rad51A1-54F11* and *rad51A1-54F11d1*, and PCR amplification with the primer pair rad51a-244 and raidp31 will be positive for *Rad51A1-B73/rad51A1-54F11* and *Rad51A1-B73/rad51A1-54F11d1* plants and negative for *rad51A1-54F11/rad51A1-54F11* and *rad51A1-54F11d1/rad51A1-54F11d1* plants (Figure 2). In addition, the primer radel is located on the region deleted in *rad51A1-54F11d1* relative to *rad51A1-54F11*; PCR amplification with the primer pair rad51a-244 and radel will be positive for *Rad51A1-B73/rad51A1-54F11d1* plants and negative for *rad51A1-54F11d1/rad51A1-54F11d1* plants.

The primer pair Mu-TIR and RB-98E7 can amplify the *Mu* insertion allele *rad51A2-98E7d4*. The primer rbdel is located on the region deleted in *rad51A2-98E7d4* relative to *rad51A2-98E7*. Hence, PCR amplification with the primer pair RB-98E7 and rbdel will be positive for *Rad51A2/rad51A2-98E7d4* plants and negative for *rad51A2-98E7d4/rad51A2-98E7d4* plants.

Irradiation of dry kernels: Irradiation was conducted at the Linear Accelerator Facility (LAF) at the Iowa State University Meat Laboratory. Kernels arising from the self-pollination of plants with the genotype (*Rad51A1/rad51A1; rad51A2/rad51A2*) were irradiated using a Circe IIIR electron beam irradiator (Linac Technologies, SA, Orsay, France) with an energy level of 10 MeV and a dose rate of 29 kGy/min. Dry kernels were placed on a conveyor cart in a single layer. Alanine dosimeters were placed on the top and bottom surfaces of these samples. Samples were exposed to the electron beam using a single-sided pass. Actual absorbed doses were measured by placing the alanine dosimeters into the e-scan electron paramagnetic resonance instrument (Bruker BioSpin). The actual dose kernels

absorbed in this treatment was 0.37 kGy delivered by an electron beam that had a dose rate of 28.8 kGy/min. Treated kernels were immediately germinated in 96-well flats. DNA was isolated from germinated seedlings (Dietrich *et al.* 2002) and their genotypes were determined via PCR.

Preparation and observation of microsporocytes: Microsporocyte samples were fixed in a freshly prepared 3:1 mixture of 95% ethanol and acetic acid (v:v) and then stored at −20°. Anthers were smeared and stained with acetocarmine following the procedure of Dempsey (1994).

Fixation and preparation of meiocytes for fluorescence *in situ* hybridization and immunostaining: Anthers were prepared following the procedure of Golubovskaya *et al.* (2002). Briefly, anthers from developing tassels were staged with the acetocarmine squash technique. Anthers from the same floret and from those in close proximity, and thus close in developmental stage, were fixed at room temperature in 4 ml of 4% formaldehyde in buffer A [15 mm PIPES, NaOH, pH 6.8, 80 mm KCl, 20 mm NaCl, 0.5 mm EGTA, 2 mm EDTA, 0.15 mm spermine tetra HCL, 0.05 mm spermidine, 1 mm dithiothreitol, 0.32 m sorbitol (Bass *et al.* 1997)] for 45 min in a gently shaking 10-ml petri dish. They were then washed three times, 30 min each in fresh buffer A, and stored at 4° in the buffer. Fixed anthers were cut open at the tip to release the meiocytes into 100–200 μl of buffer A. Ten microliters of meiocytes suspended in the buffer A were then transferred by micropipette onto a glass cover slip (22 × 22 mm) followed by the immediate addition of 5 μl of activated acrylamide stock. Acrylamide was activated by the addition of 5 μl of 20% ammonium persulfate and 5 μl of 20% sodium sulfite to 100 μl of a 15% (29:1 acrylamide:bis acrylamide) gel stock in 1× buffer A. Slides were quickly stirred and a second cover slip was placed on top for 45 min, then removed with a razor blade, leaving a thin pad of acrylamide with embedded meiocytes on the slide.

Probes: A 27-bp oligonucleotide, 5′-CCTAAAGTAGTGGATTGGGCATGTTCG-3′, labeled with either Cy5 or FITC, was obtained from Genset (Paris) and was used to detect the CentC sequence that resides near maize centromeres (Ananiev *et al.* 1998). Oligonucleotides complementary to the telomere repeat (5′-{CCCTAAA}$_4$-3′) and labeled with either Cy5 or FITC (Genset) were used to detect maize telomeres (Bass *et al.* 1997). A 5S rDNA probe was made by PCR. Approximately 1–10 ng of a plasmid containing 5S rDNA sequence from maize (Zimmer *et al.* 1988) was added to a standard PCR reaction mix: 2 μl 10× buffer with 15 mm $MgCl_2$ from Perkin-Elmer, 2 μl of forward and reverse primers, 2 μl 1 mm dATP, dGTP, dCTP, a mixture of dTTP and dUTP-FITC or dUTP-Cy5, 2 units AmpliTaq (Perkin-Elmer), and water to 20 μl. For each labeling reaction, a 20 μl unlabeled control reaction was performed, and an aliquot of equal molar volume was run side by side with the labeling reaction in a 4% gel. Incorporation of fluorescent label could sometimes be seen on the transilluminator, but empirical determination of probe effectiveness by fluorescence *in situ* hybridization (FISH) was required for each batch of probe.

FISH and indirect immunofluorescence: FISH was performed following the procedure of Golubovskaya *et al.* (2002). Briefly, newly polymerized acrylamide pads were washed with 1× PBS, followed by four washes with a prehybridization buffer (50% deionized formamide, and 2× SSC). Cover slips were placed on a slide, then 50 μl of probe in prehybridization buffer was added, then sealed under a second cover slip using rubber cement, and incubated at 37° for 30–45 min. Slides were denaturated on a PCR block at 96° for 6 min followed by overnight incubation at 30°. Slides were then washed for 30 min sequentially with 1× PBS and 1× SSC (three times), 1× PBS and 0.1% Tween-20 (four times), 1× PBS (three times), 1× TBS (one time). Slides were then stained with 10 μg/ml DAPI (4′,6-diamidino-2-phenylindole, dihydrochloride) in 1× TBS for 30 min at room temperature. Excess DAPI was removed by washing with 1× TBS (three times) for a total of 30 min. Slides were then mounted in 1,4 diazabicyclo-[2,2,2] octane (DABCO) and sealed with clear fingernail polish and stored at 20°. The procedure for staining RAD51 foci using the anti-HsRAD51 rDNA antibody was as described previously (Franklin *et al.* 1999).

Three dimensional deconvolution light microscopy and image generation: Images were acquired on a Delta Vision (Applied Precision) imaging station: an Olympus IX70 inverted microscope with 100×, 1.35 NA oil-immersion lens and a photometric (Roper Scientific) CCD. All images were taken with a Z step size of 0.2 μm, saved as 3-D stacks, and subjected to constrain iterative deconvolution. Three-dimensional data analysis and two-dimensional image creation were performed using the DeltaVision/Soft WoRx software package (Applied Precision) on a Silicon Graphics work station. Two-dimensional images were converted to TIFF and opened in Photoshop on a Macintosh computer. Photoshop was used to manipulate false colors and to convert colors from RGB to CMYK for printing.

RESULTS

Structures of the *rad51A1* and *rad51A2* genes: The maize genome contains two homologs of the yeast *rad51* gene: *Zmrad51A1* and *Zmrad51A2*, which map to chromosomes 7 and 3, respectively (Franklin *et al.* 1999). These two genes are most closely related to *AtRAD51* and only distantly related to *AtRAD51* paralogs (*AtRAD51B*, *AtRAD51C*, *AtRAD51D*, *AtXRCC2*, and *AtXRCC3*; Bleuyard *et al.* 2005; Figure 1). Full-length cDNA sequences of each gene have been reported previously (GenBank accession nos. AF079428 and AF079429). The structures of the *Zmrad51A1* and *Zmrad51A2* genes were constructed on the basis of alignments of these apparently full-length cDNA sequences with assembled genome survey sequences (GSSs) supplemented by additional sequencing of a *Zmrad51A1* genomic clone (Figure 2).

Analysis of *rad51* copy number in the maize genome: The coding regions of *rad51A1* and *rad51A2* are 84 and 90% identical at the nucleotide and amino acid levels, respectively. DNA gel blot analysis was conducted to determine the number of *rad51* genes in the maize genome. When the final wash was performed at 65°, the *rad51A1* (supplemental Figure 1, lane 1, at http://www.genetics.org/supplemental/) and *rad51A2* (supplemental Figure 1, lane 3) cDNA probes are gene specific. Under less stringent wash conditions (55°) the *rad51A1* cDNA probe detects fragments derived from both the *rad51A1* and *rad51A2* genes (supplemental Figure 1, lane 2), but no other strongly hybridizing fragments. Consistent with DNA gel blot results, the MAGI maize genomic (http://magi.plantgenomics.iastate.edu/) and EST databases do not contain another gene that is highly similar to *rad51A1* or *rad51A2* (using a cut-off value of 75% nucleotide identity). In summary, these results indicate that there are only two *rad51* genes in the maize genome.

Isolation of *Mu*-insertion alleles of *rad51A1* and *rad51A2*: Three *Mu*-insertion alleles of *rad51A1* (*rad51A1-42A8*, *rad51A1-54F11*, and *rad51A1-family6*) and two of

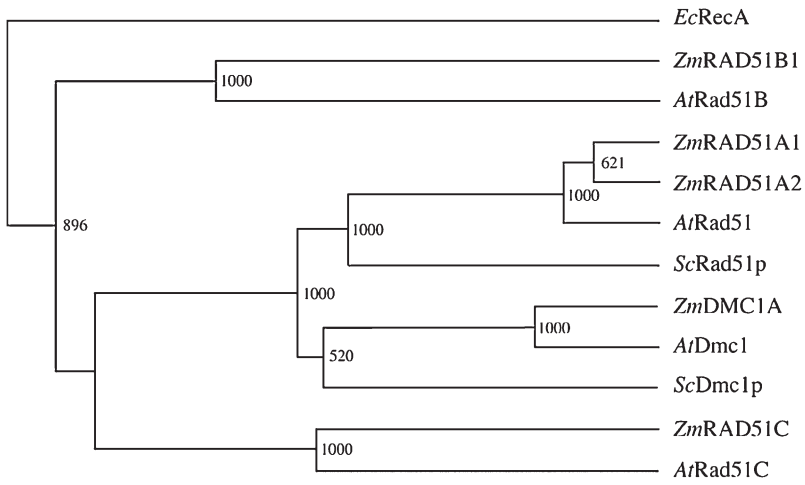

FIGURE 1.—A phylogenetic tree of selected RecA-like proteins of maize, Arabidopsis, and yeast. This average distance tree was generated using the clustalx1.83 and viewed with njplot. Statistical support for this phylogenetic tree was assessed by bootstrap analysis using 1000 replicate data sets. The relevant bootstrap value is shown at each node. *Ec*, *Escherichia coli*; *Zm*, *Zea mays*; *At*, *Arabidopsis thaliana*; *Sc*, *Saccharomyces cerevisiae*. From top to bottom, GenBank accession numbers are V00328, DT947589, AY820160, AF079428, AF079429, NM_122092, M88470, BM501047, NM_113188, P25453, BD270520, NM_130091.

rad51A2 (*rad51A2-63H3* and *rad51A2-98E7*) were recovered via the reverse genetic screen TUSC (BENSEN *et al.* 1995).

Of the five TUSC alleles, only one, *rad51A1-54F11*, contained a *Mu* transposon insertion in a coding region (Figure 2). The other alleles had insertions in introns or 5′ of the apparent transcription start sites. Because such alleles might confer residual gene function and might also be subject to "*Mu* suppression" (BARKAN and MARTIENSSEN 1991; MARTIENSSEN and BARON 1994; CUI *et al.* 2003;), they were not considered ideal reagents for the study of RAD51 functions.

Deletion derivatives of *rad51A2-98E7*: Although germinal excision events are recovered only rarely from

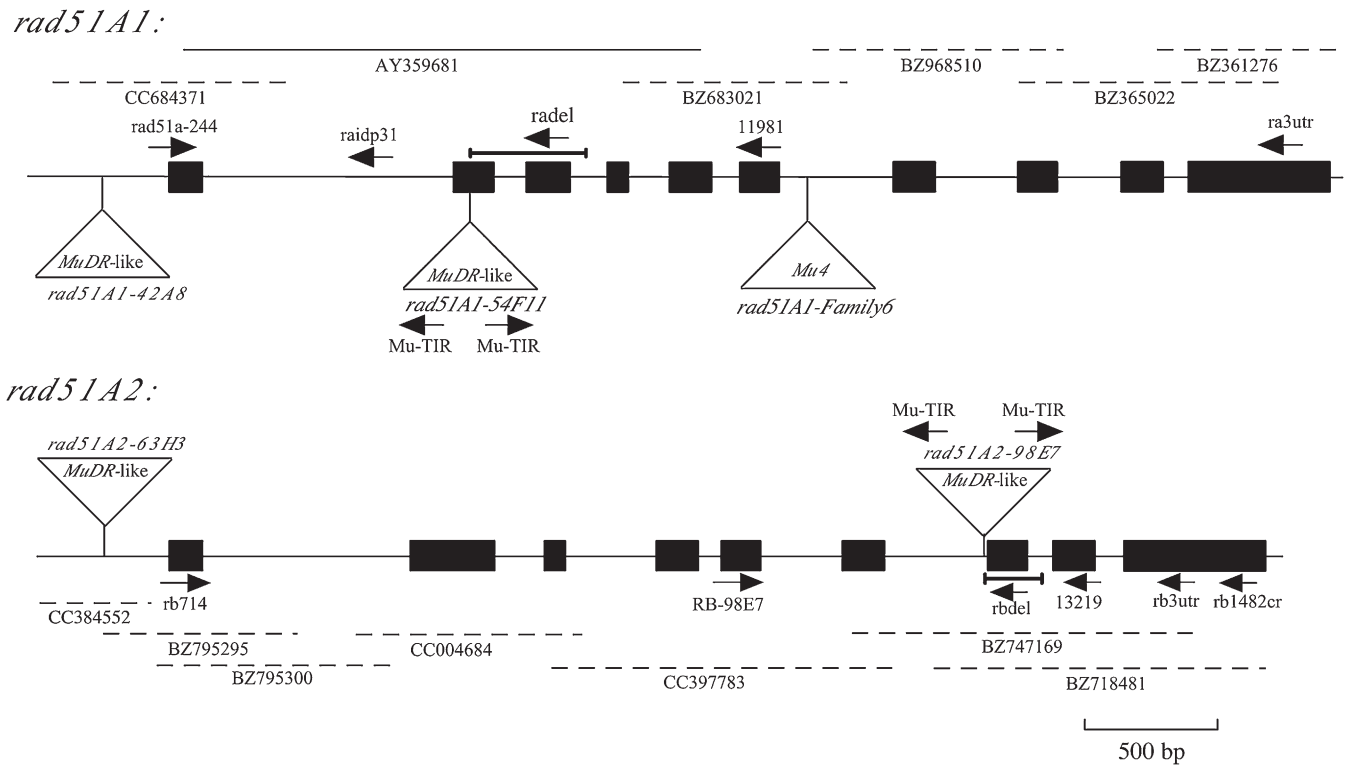

FIGURE 2.—Structures of the *rad51A1* and *rad51A2* genes. Exons are represented by boxes. The splice sites of *rad51A1* and *rad51A2* are conserved except that exon II of *rad51A2* is split into two exons (II and III) in *rad51A1*. *Mu* insertions in TUSC alleles are indicated by triangles. The class of *Mu* element is indicated in each case. The positions of oligonuleotides are indicated with arrows. The horizontal dotted and dot-dash lines represent GSSs obtained from methylation-filtered and high Cot libraries, respectively. GenBank accession numbers are indicated for each GSS. The portion of the *rad51A1* genomic sequence (GenBank accession no. AY359681) that fills the gap between CC684371 and BZ683021 was subcloned from a B73 *Rad51A1* genomic phage clone. The thick horizontal lines above exons II and III of *rad51A1* and below exon VII of *rad51A2* designate the deleted portions of *rad51A1-54F11d1* and *rad51A2-98E7d4*, respectively. There are no *Bgl*I sites in either gene.

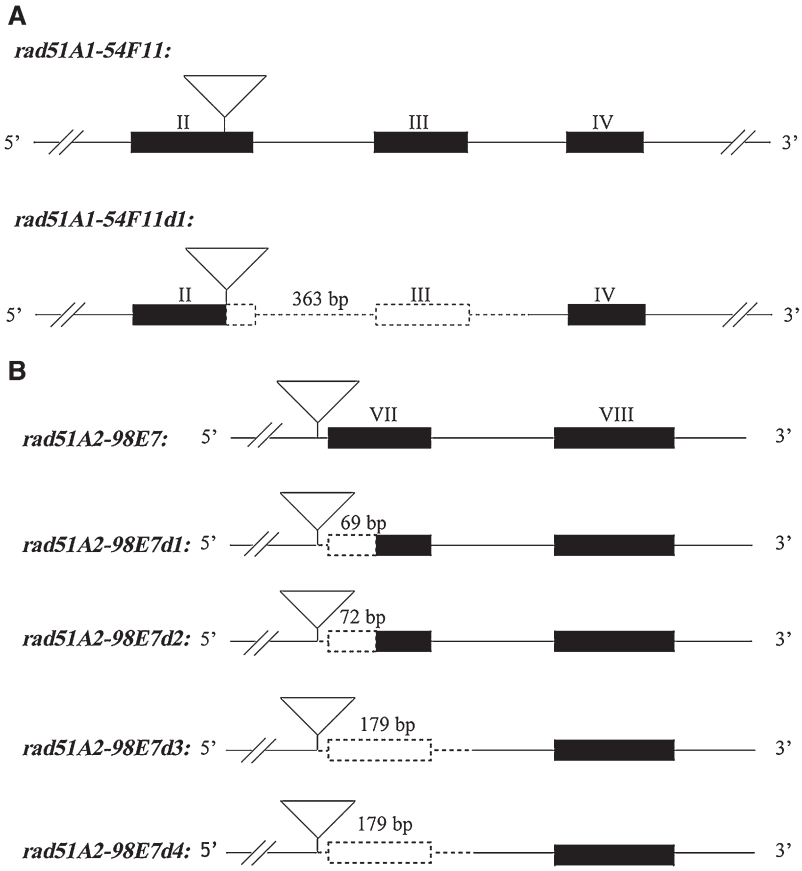

FIGURE 3.—Structures of *rad51A1-54F11* and *rad51A2-98E7* deletion derivatives. Shaded boxes represent exons; *Mu* insertions are designated by triangles. The 5′ end of each deletion is located at a *Mu* insertion site. Deleted regions are designated by dashed lines and the size of each deletion is indicated in base pairs. Each deletion derivative was isolated from an independent cross. Hence, although d3 and d4 arose via identical deletions, they must have arisen via independent events. (A) *rad51A1-54F11* and its deletion derivative, *rad51A1-54F11d1*. (B) *rad51A2-98E7* and its deletion derivatives.

Mu-insertion alleles (BROWN *et al.* 1989; LEVY *et al.* 1989; SCHNABLE *et al.* 1989), ~1% of gametes carry deletions adjacent to a given *Mu* insertion (TAYLOR and WALBOT 1985; LEVY and WALBOT 1991; DAS and MARTIENSSEN 1995). A PCR-based screen modified from that described by DAS and MARTIENSSEN (1995) was used to identify rare derivatives of *rad51* TUSC alleles that contained deletions adjacent to the *Mu* insertions.

The *rad51A2-98E7* allele was selected to screen for deletions because its *Mu* insertion is located near an intron–exon junction. Initially, *rad51A2-98E7* was crossed into a *Mu* active line (cross 1, MATERIALS AND METHODS). Progeny of this cross that carried *rad51A2-98E7* were crossed by the inbred line B73 (cross 2); ~1000 of the resulting progeny were germinated and analyzed via PCR using the Mu-TIR primer in conjunction with the gene-specific primer 13219. Seedlings that yielded smaller PCR products than those obtained from *rad51A2-98E7* were grown to maturity and backcrossed to B73. The progeny from these crosses were genotyped via PCR; four heritable derivative alleles were recovered (Figures 2 and 3).

Experiments conducted as described in MATERIALS AND METHODS indicated that all four of the heritable derivative alleles arose via adjacent deletions (data not shown). Sequence analysis of the PCR products associated with these alleles established that the sizes of the deletions range from 69 to 179 bp (Figure 3). In the case of deletion derivative *rad51A2-98E7d4*, all of exon VII has been deleted. Because only half of the progeny from cross 2 would be expected to carry *rad51A2-98E7*, the rate at which adjacent deletions were recovered from *rad51A2-98E7* was ~0.8% (4/~500).

A deletion derivative of *rad51A1-54F11*: The *rad51A1-54F11d1* deletion derivative was isolated from a family segregating for *rad51A1-54F11* (MATERIALS AND METHODS). Sequence analysis of a PCR product amplified from *rad51A1-54F11d1* established that the 363 bp (~1447–1809 in GenBank accession no. AY359681) that was deleted includes part of exon II, all of intron II and exon III, and part of intron III (Figure 3).

RT–PCR analysis of *rad51* double mutants: RT–PCR experiments were conducted to test whether the *rad51A1* and *rad51A2* deletion derivative alleles are null mutants. Consistent with observations of FRANKLIN *et al.* (1999), *rad51A1* and *rad51A2* transcripts of the expected sizes were detected during meiotic prophase in maize tassels that carry *Rad51A1* and *Rad51A2*, respectively (Figure 4). In contrast, *rad51A1* transcripts were not detected in plants homozygous for *rad51A1-54F11d1*. Hence, *rad51A1-54F11d1* is an apparently null mutant allele.

Expression of the *rad51A2-98E7d4* was analyzed similarly. Although ethidium bromide staining of the RT–PCR products did not reveal any *rad51A2* transcripts in plants homozygous for *rad51A2-98E7d4*, RT–PCR products of two transcripts could be detected via hybridization with a *rad51A2* cDNA probe (data not shown). Sequence

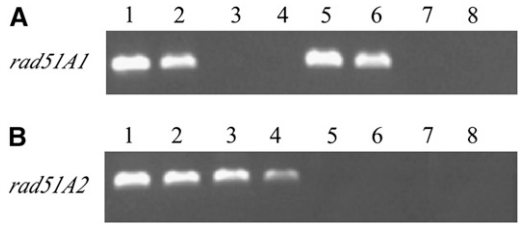

FIGURE 4.—RT–PCR analysis of *rad51A1* and *rad51A2*. RNA was isolated from tassels undergoing meiotic prophase from plants with the following genotypes: homozygous for *Rad51A1* and *Rad51A2* (lanes 1 and 2), homozygous for *rad51A1-54F11d1* and *Rad51A2* (lanes 3 and 4), homozygous for *Rad51A1* and *rad51A2-98E7d4* (lanes 5 and 6), and homozygous for *rad51A1-54F11d1* and *rad51A2-98E7d4* (lanes 7 and 8). Gene-specific PCR primers that flank the *Mu* insertions and more than one intron were used to amplify first-strand cDNAs. PCR products were resolved via agarose (0.8%, w/v) gel electrophoresis and visualized with ethidium bromide. (A) RT–PCR analysis of *rad51A1*. First-strand cDNAs were amplified with the primer pair rad51a-244 and 11981 (Figure 2). (B) RT–PCR analysis of *rad51A2*. First-strand cDNAs were amplified with the primer pair RB-98E7 and rb3utr (Figure 2).

analysis demonstrated that one of these transcripts is missing all of exon VII as expected on the basis of the structure of *rad51A2-98E7d4* (Figures 2 and 3). The deletion of exon VII causes a frameshift in this transcript. The second transcript is also missing exon VII but includes 142 bp from the TIR of the *MuDR* transposon. In this transcript, a stop codon has been introduced before exon VIII. Hence, in both transcripts ~ 80 amino acids of the normal RAD51A2 protein, including a large portion of the ATP binding site (SHINOHARA *et al.* 1992; NARA *et al.* 2000), are lost due to deletions, frameshift, or a premature stop codon. Hence, it is very unlikely that *rad51A2-98E7d4* encodes a functional protein.

The *rad51* double mutant does not accumulate RAD51 foci: To further test whether *rad51A1-54F11d1* and *rad51A2-98E7d4* are null alleles, meiocytes from wild type and *rad51* double mutants were subjected to immunolocalization using RAD51 polyclonal antibodies (FRANKLIN *et al.* 1999). In wild type, RAD51 appears on chromosomes as distinct foci and reaches a maximum of 500–600 foci in mid-zygotene (FRANKLIN *et al.* 1999; Figure 5A). In contrast, true RAD51 foci were not observed in *rad51* double mutant cells (Figure 5B). This dramatic difference, together with RT–PCR results (Figure 4), demonstrates that the *rad51A1-54F11d1* and *rad51A2-98E7d4* alleles do not encode functional RAD51.

RAD51 is essential for the repair of radiation-induced DSBs during vegetative development: To address the role of RAD51 in DNA repair during early vegetative development, ~200 dry kernels that were segregating for *rad51* double mutants were irradiated with a dose of 0.37 kGy prior to germination. While control siblings survived to develop into apparently healthy seedlings, all the *rad51* double mutants ($N = 31$) germinated 3–4 days later than control siblings, were able to produce only one leaf, and died within 2 weeks of germination (Table 1). This result indicates that RAD51 function is essential for the repair of radiation-induced DSBs in maize.

Effects of *rad51* double mutants on gamete production: Plants homozygous for *rad51A1-54F11*, *rad51A1-54F11d1*, or *rad51A2-98E7d4* (*i.e.*, single mutants) develop apparently normally, are fully male fertile, and have normal seed sets. To determine whether the *rad51* double mutant exhibits a phenotype, the progeny resulting from the self-pollinations of plants heterozygous for *rad51A1-54F11* or *rad51A1-54F11d1* and homozygous for *rad51A2-98E7d4* were genotyped and scored for male and female fertility. Among the progeny of these crosses, all double mutant plants were male sterile (*i.e.*, that had anthers that failed to exert and that contained no morphologically normal pollen grains) and exhibited dramatic reductions in female seed sets (Table 2 and Figure 5, C and D). When crossed as females (*i.e.*, serving as pollen recipients) with wild-type pollen, 14 *rad51* double mutants produced 800 kernels, while six control wild-type siblings produced 1555 kernels. Hence, in this experiment, seed set of *rad51* double mutants was ~22% ($(800/14)/(1555/6) \times 100\% = 22\%$) of wild type. In all other respects double mutant plants developed apparently normally.

Reduced number of bivalents and chiasmata in *rad51* double mutants: Meiosis was analyzed using acetocarmine squashes in microsporocytes of plants that were wild type, homozygous for either of the two single mutations (*i.e.*, *rad51A1/rad51A1; Rad51A2/Rad51A2* or *Rad51A1/Rad51A1; rad51A2/rad51A2*) or the *rad51* double mutant. The meiotic sequence appeared to be normal in both of the *rad51* single mutant genotypes.

At diakinesis the average number of bivalents per wild type and *rad51* double mutant cell was 10 (10.0 ± 0.1) and 4.1 ± 2.1, respectively (Table 3, Figure 6, A–D). To determine the number of chiasmata, the numbers of ring-shaped bivalents, which have two chiasmata, and rod-shaped bivalents, which have one chiasma, were counted (Figure 6). In *rad51* double mutants, most of the bivalents are rod shaped, indicating a decrease in the number of chiasmata per bivalent. In *rad51* double mutants, the average number of chiasmata per bivalent is 1.0 ± 0.3, while in wild type it is 1.9 ± 0.1 (Table 3). Although the average number of chiasmata per double mutant cell is only 4.5 ± 2.5 (as compared to 20 in normal cells), the existence of chiasmata suggests that some degree of recombination and synapsis occurs in the absence of RAD51.

Chiasmata between nonhomologous chromosomes in *rad51* double mutants: A unique and significant feature of the *rad51* double mutants was discovered while counting chiasmata in metaphase I cells. In addition to univalents and bivalents, multivalents (trivalents and quadrivalents) and heteromorphic bivalents were observed in the *rad51* double mutants (Figure 6, E–H). Heteromorphic bivalents have been studied in wheat and interspecies hybrids and multivalents can be easily

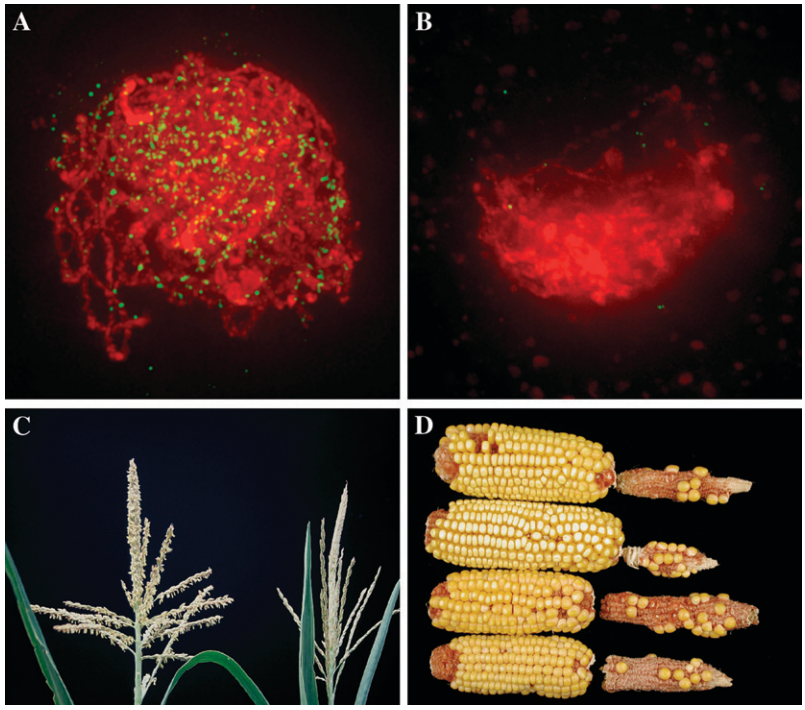

FIGURE 5.—RAD51 foci in zygotene cells and phenotypes of *rad51* double mutant. RAD51 immunostaining is shown in green and DAPI stained chromosomes are in red. (A) Wild-type nucleus showing hundreds of distinct RAD51 foci. (B) A *rad51* double mutant nucleus showing very few, if any, foci. Because the few green dots have intensities far below those of normal RAD51 foci, they are probably background. (C) Effect on male fertility. The plant shown on the left had the genotype *rad51A1-54F11/Rad51A1; rad51A2-98E7/rad51A2-98E7d4* and was fully fertile. The plant shown on the right was homozygous for *rad51A1-54F11* and *rad51A2-98E7d4* and was completely male sterile. The same phenotype was observed when *rad51A1-54F11d1* was substituted for *rad51A1-54F11*. To further check the viability of male gametes from *rad51* double mutants, five anthers were dissected from each male sterile plant. These anthers were then cut into small pieces and placed directly on female silks of B73 plants. No seed was set from 10 such crosses. (D) Effect on female fertility. Ears on the left were generated via self-pollination of plants with the genotype *rad51A1-54F11/Rad51A1; rad51A2-98E7d4/rad51A2-98E7d4*. Ears on the right were generated by crossing plants homozygous for *rad51A1-54F11* and *rad51A2-98E7d4* as females by plants with the genotype *rad51A1-54F11/Rad51A1; rad51A2-98E7d4/rad51A2-98E7d4*. These seed sets were similar to those obtained via open pollination. The same effects on female fertility were observed when *rad51A1-54F11d1* was substituted for *rad51A1-54F11*.

seen in translocation heterozygotes in maize, and both have characteristic morphology. A heteromorphic bivalent appears as two chromosomes of different sizes held together at metaphase I by chiasmata (Figure 6H). Although it is possible that this is the result of a homologously paired bivalent that has suffered breakage, we consider this unlikely because the breakage would have to involve both sister chromatids. Even more convincing evidence of chiasmata between nonhomologous chromosomes comes from the multivalents, which appear as three or four chromosomes forming chain-shaped (Figure 6, E and G) or ring-shaped (Figure 6F) quadrivalents. The frequency of multivalent and heteromorphic bivalents was ~6%: among 82 metaphase I cells analyzed, only one heteromorphic bivalent and four multivalents were found (Figure 6). Thus, the nonhomologous synapsis observed in pachytene sometimes allows for chiasmata between nonhomologous chromosomes. Chiasmata between nonhomologous chromosomes do not occur in any other pairing-defective maize meiotic mutants that have been analyzed, even those with elevated levels of nonhomologous synapsis, such as *phs1* (I. N. GOLUBOVSKAYA, data not shown, and PAWLOWSKI *et al.* 2004). This indicates that in the absence of RAD51, nonhomologous chromosomes can synapse. To our knowledge, multivalents and heteromorphic bivalents have

TABLE 1

RAD51 is required for the repair of radiation-induced DSBs

Genotype[a]	Fraction of seedlings surviving 2 weeks after germination[b]
rad51A1/rad51A1	0/31
Rad51A1/rad51A1	97/97[c]
Rad51A1/Rad51A1	55/55

[a] All seedlings were homozygous for *rad51A2-98E7d4* and segregated for *rad51A1-54F11d*.

[b] Kernels obtained via self-pollinations of plants heterozygous for *rad51A1-54F11d1* and homozygous for *rad51A2-98E7d4* were irradiated, germinated, and genotyped. The five kernels that failed to germinate are not included.

[c] Two seedlings were less than half normal height and had aberrantly shaped leaves.

TABLE 2

Correlation between male sterility and the *rad51* double mutant

	Fraction of progeny with the indicated genotypes that were male sterile[b]	
rad51A1 genotype[a]	*rad51A1-54F11*	*rad51A1-54F11d1*
rad51A1/rad51A1	12/12	12/12
Rad51A1/rad51A1	0/25	0/24
Rad51A1/Rad51A1	0/11	0/6

[a] All plants were homozygous for *rad51A2-98E7d4*.

[b] Progeny obtained via self-pollinations of plants heterozygous for the indicated allele of *rad51A1*.

TABLE 3

Average number of bivalents and chiasmata per diakinesis cell in *rad51* double mutants and wild type control

Genotype	No. bivalents per cell	No. chiasmata		No. cells analyzed
		Per cell	Per bivalent	
rad51 double mutant[a]	4.1 ± 2.1	4.5 ± 2.5	1.0 ± 0.3	78
Wild type[b]	10.0 ± 0.1	19.0 ± 1.0	1.9 ± 0.1	72

[a] Based on analyses of two *rad51* double mutant plants.
[b] Based on analyses of two samples of the inbred line A344.

been observed only in the *ph1* mutant of common wheat, where homeologous chromosomes can synapse (in addition to homologous chromosomes), recombine, and form chiasmata (Riley and Chapman 1964; Riley *et al.* 1966) and Arabidopsis *zyp1* mutants (Higgins *et al.* 2005).

Chromosome breaks from male meiocytes in *rad51* double mutants: The first indication of chromosome breakage in the *rad51* double mutants was seen at diakinesis and metaphase I. Numerous chromosome fragments are evident at anaphase I, indicating a high degree of chromosome breakage in the *rad51* double mutants (Figure 7). Of 35 anaphase I cells specifically analyzed for breakage (and in hundreds of other cells looked at for other purposes), all showed chromosome breakage. Different sizes of chromosome fragments range from a whole chromosome arm to tiny, single, and double fragments. This is very unusual in maize, where chromosome breaks in other meiotic mutants are "healed" by late pachytene (Pawlowski *et al.* 2004). In addition to chromosome breaks, abnormal stretches of chromosomes are seen at anaphase I (Figure 7, B–F). These appear broken randomly throughout the spindle. These are distinguished from classical chromosome bridges, which are also observed in *rad51* double mutants at anaphase II accompanied by fragments (Figure 7J). Classical chromosome bridges (as in Figure 7J), resulting from dicentric chromosomes being pulled to two poles at anaphase I, span the distance from one daughter nucleus to the other, are very stable, and are usually broken only by the phragmoplast (as can be seen in Figure 7I).

RAD51 is required for normal meiotic disjunction: The meiotic abnormalities observed in the *rad51* double mutant would be expected to affect meiotic chromosome segregation. Quartets of microspores were examined in eight *rad51* double mutant plants. In normal maize plants, one nucleolus is present in each of the four microspores of each quartet because each microspore contains only one copy of chromosome 6, which carries the only nucleolar organizing region (NOR) (McClintock 1934). Many of the quartets contained one or two microspores that lacked an organized nucleolus (Figure 8A) but contained numerous micronucleoli (smaller bodies that resembled nucleoli, Figure 8, B–F). Because two nucleoli can fuse together, the types of aberrant quartets illustrated in Figure 8, B–D, could arise via nondisjunction or loss of chromosome 6 in one or more cells. Microspores that contained two nucleoli (Figure 8, E and F) have two copies of chromosome 6. The observed frequencies of the various types of quartets in four of the double

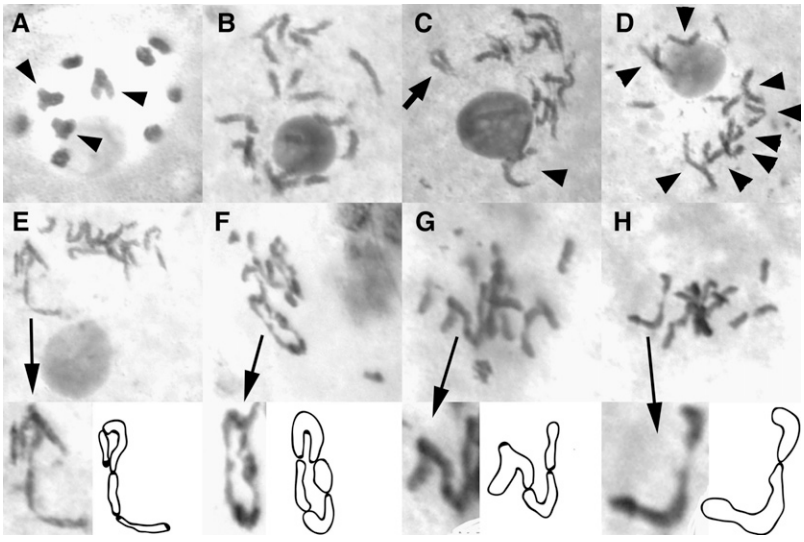

Figure 6.—Bivalents and multivalents in *rad51* double mutants at diakinesis. Male meiocytes from wild type (A) or from *rad51A1-54F11d1/rad51A1-54F11d1; rad51A2-98E7d4/rad51A2-98E7d4* (B–H) were stained with acetocarmine and observed under light microscopy. (A) Wild-type diakinesis showing 10 bivalents: 7 closed (two chiasmata per bivalent) and 3 open (one chiasma per bivalent, arrowheads). (B) With 20 univalents, thus zero chiasmata. (C) With 1 open bivalent (arrowhead) showing one chiasma, and 1 closed bivalent (arrow) with two chiasmata. (D) With 8 rod bivalents (arrowheads) and 4 univalents, thus 8 chiasmata in this nucleus. (E) One nucleus with a quadrivalent, enlarged (bottom) with a cartoon of each chromosome. (F) One nucleus with a ring-of-four quadrivalent, enlarged (bottom) with a cartoon of each chromosome. (G) One nucleus with a trivalent, enlarged (bottom) with a cartoon of each chromosome. (H) One nucleus with a heteromorphic bivalent, enlarged (bottom) with a cartoon.

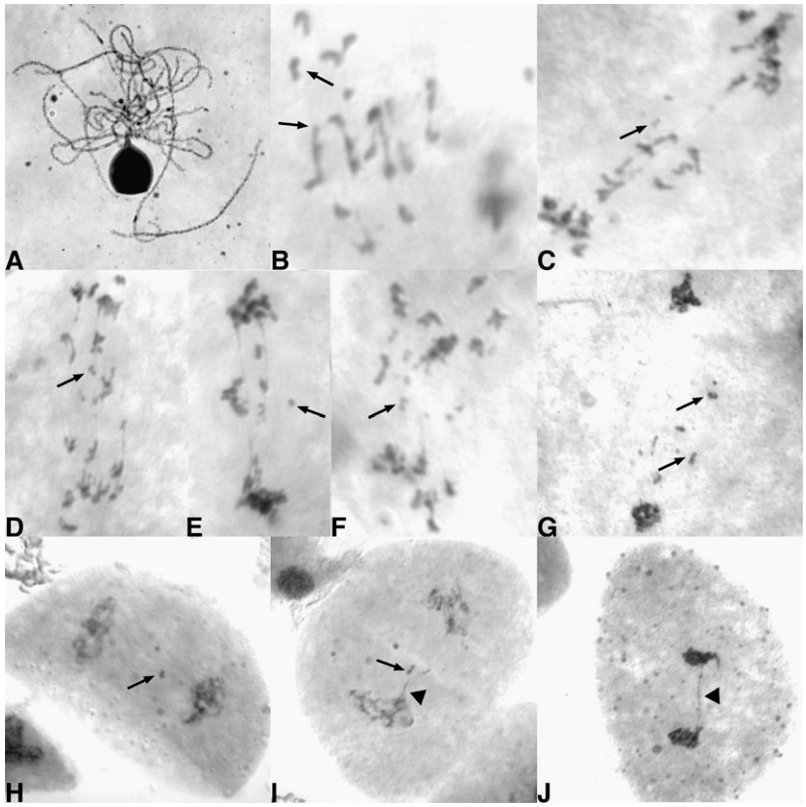

FIGURE 7.—Chromosome breakage and bridges occur in *rad51* double mutants. These are acetocarmine chromosome squashes of *rad51* double mutant meiocytes in pachytene through telophase II. (A) Pachytene looks completely normal at this level of examination. (B) Metaphase I with a broken chromosome arm (top arrow), and as a result of this breakage the top chromosome of the bivalent is now telocentric (bottom arrow). (C–G) Different sizes and numbers of fragments are seen in anaphase I (C–F) and in telophase I (G) (examples indicated by arrows). (H–J) Chromosome fragments (arrow) and bridges (arrowhead) are seen at telophase II. Bridges are seen only in the second meiotic division.

mutant plants are provided in Table 4. Because cells with two nucleoli possess two copies of chromosome 6, the abnormal quartet types observed in the *rad51* double mutant in this study could be produced only if chromosome 6 underwent nondisjunction at one of the meiotic divisions. For example, quartet type VIII (Table 4) could be produced only via nondisjunction of chromosome 6 during the first meiotic division. Similarly, quartet types III and IV (Table 4) could be produced only via nondisjunction of chromosome 6 during the second meiotic division. Hence, *rad51* function is required for the normal disjunction of chromosome 6 (and presumably the other chromosomes) during both meiotic divisions.

Meiotic homologous pairing is reduced in the *rad51* double mutants: Even though chromosome pairing at pachytene in *rad51* double mutants looks indistinguishable from wild-type plants at the light microscope level (Figure 7A), we wanted to determine if the abnormalities observed from metaphase I to quartet stage were a consequence of an earlier meiotic malfunction. The degree of homologous pairing in *rad51* double mutants was assessed using FISH with a 5S rDNA probe that hybridizes to a single locus in maize (GOLUBOVSKAYA *et al.* 2002). Since maize is diploid, two FISH foci are seen if homologous pairing has not occurred and only one if pairing is complete. In wild type at pachytene, 100% of cells show one single, bright 5S rDNA focus, indicating

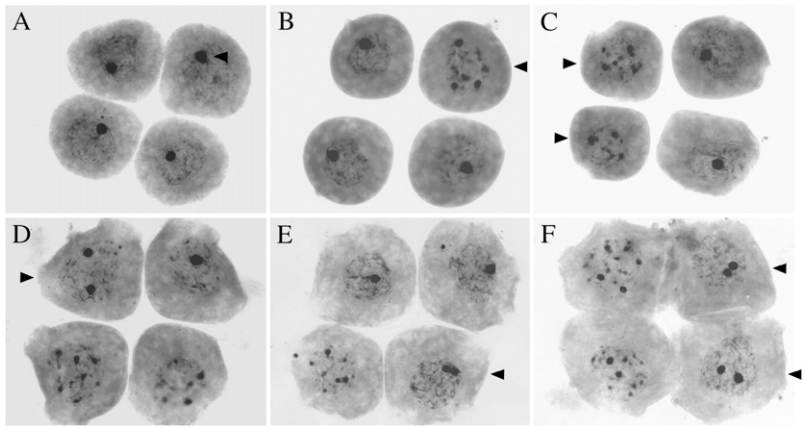

FIGURE 8.—Types of quartets observed from *rad51* double mutants. Normal (A) and abnormal (B–F) quartets. The arrowhead in A indicates an organized nucleolus. The arrowheads in B and C indicate microspores missing an organized nucleolus. The arrowheads in D, E, and F indicate microspores with two organized nucleoli.

TABLE 4

Frequencies of quartet types in *rad51* single and double mutants

	rad51A1: *rad51A2*:	Mutant[a] Mutant				Mutant Wild type		Wild type[b] Mutant	
Quartet type[c]	Plant ID:	01-2992-5	01-2996-8	05B-2886-16	05B-2886-4	01-1004-1	01-1002-2	01-1009-1	01-1009-2
I		60	50	84	71	78	80	80	80
II		15	21	12	13	0	0	0	0
III		2	3	6	3	0	0	0	0
IV		0	2	3	4	0	0	0	0
V		3	3	4	6	0	0	0	0
VI		8	10	11	14	0	0	0	0
VII		0	1	2	2	0	0	0	0
VIII		1	2	6	8	0	0	0	0
Abnormal quartets[d] (%)		33	43	34	41	0	0	0	0

[a] Homozygous for a mutant allele of the indicated gene. Results reported use *rad51A1-54F11* and *rad51A2-98E7d4*. Similar results were obtained when *rad51A1-54F11*d1 was substituted for *rad51A1-54F11*. All ($N = \sim 80$) quartets examined from the inbred line B73 (homozygous for *Rad51A1* and *Rad51A2*) were quartet type I.

[b] Homozygous for a wild-type allele of the indicated gene.

[c] Black spots represent organized nucleoli; open circles represent cells with multiple micronucleoli.

[d] The total percentage of observed abnormal quartets (types II–VIII).

that homologous pairing has occurred. In 41 *rad51* double mutant pachytene meiocytes, 18 (44%) had a single focus as in wild type (Figure 9A) and 23 (56%) had two unpaired foci, indicating a lack of homologous pairing. Of these 23 cell with unpaired 5S rDNA foci, 14 (34% of total) had two foci on chromosomes that were closely appressed (*i.e.*, apparently synapsed) to a nonhomologous chromosome (Figure 9B), and 9 (22%) had two very close, but unpaired foci on short stretches of unpaired chromosomes (Figure 9C). These data indicate that while homologous pairing is possible in the *rad51* double mutant, it is not nearly as efficient as in wild type. The reduced frequency of correct homologous pairing (44% of normal) correlates well with the reduced degree of bivalents (40%) in *rad51* double mutants. In addition, the apparent synapsis between nonhomologous chromosomes (Figure 9B) also correlates with the presence of multivalents and heteromorphic bivalents (Figure 6, E–H).

Nonhomologous synapsis is evident in the *rad51* double mutants: To assess the integrity of synapsis in the *rad51* double mutants, double immunolocalizations were performed with antibodies against AFD1 and ASY/HOP1. AFD1 is the maize REC8 homolog and marks both axial (before synapsis) and lateral (after synapsis) elements of the synaptonemal complex. When meiocytes are fixed in 4% formaldehyde and buffer A, AFD1/REC8 marks lateral elements more strongly. ASY1/HOP1 is an antibody toward the Arabidopsis HOP1 homolog, and in maize meiocytes fixed in 4% formaldehyde it marks only the unsynapsed axial elements (Golubovskaya *et al.* 2006). Thus, together, these antibodies can show regions where chromosomes are synapsed and unsynapsed. In wild type at pachytene, only AFD1/REC8 stains chromosomes (Golubovskaya *et al.* 2006). To examine whether synapsis is defective in *rad51* double mutants, pachytene meiocytes were selected by their appearance of the chromosomes in the DAPI channel. In deconvolution microscopy, this can easily be determined because synapsed chromosomes are exactly twice the width of chromosomes at leptotene, when chromosomes are completely unpaired. Looking at the whole nuclei, *rad51* double mutants look normal at zygotene and pachytene (Figure 10, A–C). However, upon close inspection of individual optical Z sections in the AFD channel, nonhomologous synapsis could be easily detected. This was evident mostly by synaptic partner switches (Figure 10, D–G). These Y-shaped structures represent two chromosomes, which synapse for some distance and then are interrupted at some point (arrows) by a partner switch. Thus, three chromosomes are involved in these structures and synapsis is nonhomologous for some distance. One to four partner switches were detected per nucleus, but there may be more because it is only possible to detect partner switches in the X–Y plane. Of 14 carefully examined cells, there was one event containing two sets of nonhomologously synapsed chromosomes forming an incomplete cross-shaped quadrivalent (Figure 10F).

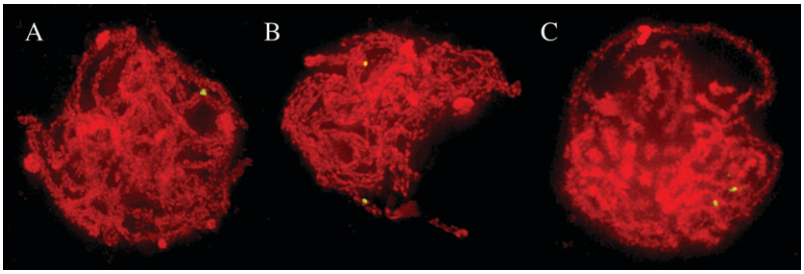

FIGURE 9.—FISH analysis of 5S rDNA loci in pachytene *rad51* double mutants meiocytes Chromosomes are shown in red (DAPI) and 5S rDNA loci in green. (A) Paired 5S rDNA foci. (B) Two unpaired 5S rDNA foci. Each 5S rDNA locus pairs with and appears to be synapsed with a nonhomologous chromosome. (C) Two close but unpaired 5S rDNA foci.

Meiotic crossovers in *rad51* double mutants: Our finding that frequency of chiasmata at diakinesis was low in male gametes of *rad51* double mutants (Table 3) is consistent with the fact that reduced chromosome pairing was observed at pachytene (Figure 9) and only ~62% quartets were normal due to aberrant segregation of chromosome 6 (Table 4).

The rates of meiotic crossovers between two genetic markers (*a1* and *et1*) were assayed in female double mutants and *rad51A2* single mutant controls. In this 10-cM interval (GOODMAN *et al.* 1980; DA COSTA E SILVA *et al.* 2004) no significant differences in the rates of crossovers were detected between *rad51* double mutants and controls (Table 5). The rates of crossovers were also measured at another genetic interval (*i.e.*, between IDP1440 and IDP1983) using an independent population. Similarly, no significant differences in the rates were detected between *rad51* double mutants and wild-type controls (Table 5). These results indicate that RAD51 is not essential for meiotic crossovers in surviving *female* meiocytes.

Further support for this conclusion comes from cytological analyses of progeny of *rad51* double mutant females pollinated with wild-type pollen. Root tips of 20 such progeny were examined cytologically; each contained the diploid number ($N = 20$) of chromosomes. Meiocytes from similarly produced progeny of *rad51* double mutant females were also examined; all had 10 pairs of chromosomes.

DISCUSSION

The two *rad51* genes are functionally redundant: Consistent with the hypothesis that maize is a segmental allotetraploid (GAUT *et al.* 2000), the maize genome contains two *rad51* homologs: *rad51A1* and *rad51A2* (FRANKLIN *et al.* 1999; supplemental Figure 1 at http://www.genetics.org/supplemental/). Apparently null or severely disrupted alleles have been isolated from both genes. On the basis of the observations that there is no evidence for more than two *rad51* genes in maize (supplemental Figure 1), that the *rad51* double mutants do not accumulate normal *rad51A1* or *rad51A2* transcripts (Figure 4), and that RAD51 foci are not detectable at zygotene (Figure 5), we conclude that the *rad51* double mutant does not exhibit residual RAD51 activity.

Plants homozygous for single mutants of either gene develop normally, are fully male fertile, and do not display

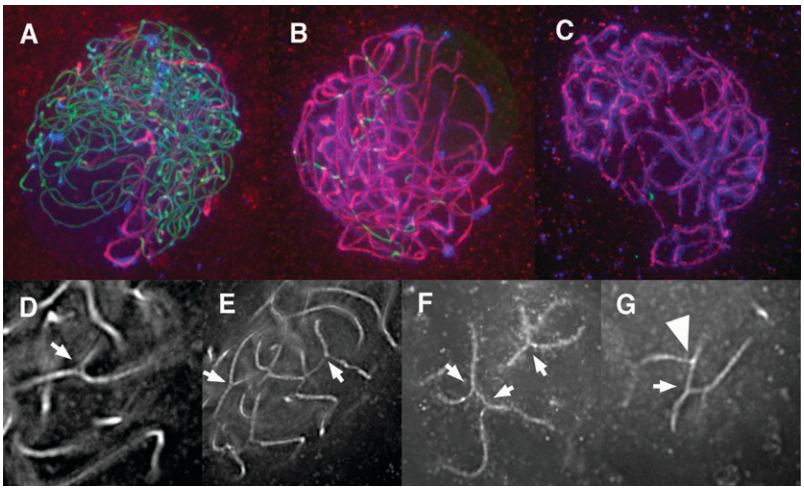

FIGURE 10.—Nonhomologous synpasis in the *rad51* double mutant. (A–C) Immunolocalization of ASY1/HOP1 (green) showing unsynapsed axial elements and AFD1 (red) showing the lateral elements of synapsed chromosome regions. DAPI stained chromosomes are shown in blue. (A) Zygotene, showing synapsed and unsynapsed chromosome regions. (B) Very late zygotene showing that almost all chromosomes are synapsed. (C) Pachytene showing complete synapsis except for a single region. At this level of resolution, these *rad51* double mutant meiocytes look completely normal. (D–G) Optical Z sections (0.2 or 0.4 μm) through the nucleus immunostained with AFD1 showing synapsed chromosomes at pachytene. Partner switches can be clearly seen. These switches indicate nonhomologous synapsis, as three chromosomes are involved, two at a time, in these Y-shaped structures. (D) A single partner switch (arrow). (E) Two different partner switches in a single section. (F) A complex partner switch, two sets of nonhomologously synapsed chromosomes forming an incomplete cross-shaped quadrivalent, and a simple partner switch. (G) Even in a single section it is possible to distinguish between a real partner switch and two overlaid chromosomes. At the arrow is a real partner switch. At the arrowhead is the bright spot where one synapsed chromosome is simply overlaid upon another. This was confirmed in 3-D.

TABLE 5

Effect of RAD51 on rates of meiotic crossovers across two intervals

Intervals	*rad51* genotype	No. kernels[a]		Genetic distance (cM) ± SE
		Parental genotypes	Recombinant genotypes	
a1–et1	Double mutant[a]	331	46	12.2 ± 1.7
	Control[b]	655	111	14.5 ± 1.3
IDP1440–IDP1983[c]	Double mutant[d]	145	20	12.1 ± 2.5
	Wild type[e]	156	26	14.2 ± 2.6

[a] Data were pooled from 12 related test crosses.

[b] Genotypes for female parents of test crosses were either *Rad51A1/Rad51A1; rad51A2/rad51A2* or *Rad51A1/rad51A1; rad51A2/rad51A2*. Data pooled from six related test crosses. These results are similar to those obtained from wild-type lines.

[c] IDP1440 and IDP1983 are PCR-based IDP markers located on the long arm of chromosome 3. Detailed information about these two markers is available from http://maize-mapping.plantgenomics.iastate.edu/idp/index.php.

[d] Data were pooled from three related crosses.

[e] These plants have the genotype *rad51A1/Rad51A1*; *rad51A2/Rad51A2* and are siblings to the *rad51* double mutants. Progeny from two related crosses are analyzed.

reduced seed set. Cytological observations do not reveal any differences between these single mutants and the inbred line B73, which carries functional alleles of both genes. In contrast, plants that are homozygous for mutant alleles at both loci are completely male sterile (Figure 5C) and exhibit dramatically reduced seed set (Figure 5D) and abnormal male meiosis (Figures 6–9). Hence, *rad51A1* and *rad51A2* appear to be functionally redundant in maize.

Roles of RAD51 in DSBs repair: This study demonstrates both significant differences and similarities in the roles of RAD51 in mitotic cells of vertebrates and plants. Consistent with the finding of Li *et al.* (2004), we demonstrate that under normal conditions, the RAD51-dependent homologous recombination repair pathway plays at best only a minor role in mitotic plant cells. In contrast, disruptions of *rad51* in vertebrates are lethal (Tsuzuki *et al.* 1996; Sonoda *et al.* 1998) due to the accumulation of unrepaired DSBs (Sonoda *et al.* 1998).

It has not previously been shown that RAD51 is involved in the repair of mitotic DSBs in plants (Bleuyard *et al.* 2006). The finding that maize *rad51* double mutant embryos are extremely susceptible to radiation-induced DSBs (Table 1) demonstrates a conserved role for RAD51 in the repair of mitotic DSBs in plants, vertebrates, and yeast.

The maize *rad51* double mutant is unique among some 20 other meiotic maize mutants in that it shows chromosome fragmentation. Most clearly established in the *phs1* mutant, meiotic chromosome breaks that are not repaired in meiotic mutants are somehow "healed" in late prophase in maize (Pawlowski *et al.* 2004). On the basis of this observation, it has been postulated that a backup DNA repair mechanism exists late in maize meiosis (Pawlowski *et al.* 2004). This is different from Arabidopsis, where many meiotic mutants show chromosome fragmentation (Bleuyard and White 2004; Li *et al.* 2004, 2005; Hamant *et al.* 2006). The maize *rad51* double mutant points to a unique and specific role of RAD51 in maize, *viz.*, it may be required for this backup repair mechanism.

RAD51 is critical but not essential for meiotic chromosome pairing, synapsis, and crossovers: The *rad51* double mutant exhibits a reduced amount of homologous pairing (44% of wild type), a reduced number of bivalents (4 *vs.* 10), and nearly completely synapsed chromosomes (Figure 10C). This is consistent with observations in yeast, in which *rad51* mutants undergo normal chromosome pairing and nearly perfect synapsis (Rockmill *et al.* 1995). Our data differ from the previous report that in Arabidopsis *rad51* plays an essential role in chromosome pairing and synapsis (Li *et al.* 2004).

The residual female fertility associated with the maize *rad51* double mutant allowed us to demonstrate that in maize, as is the case for yeast (Shinohara *et al.* 1992, 1997), rates of meiotic crossovers in the absence of RAD51 are not statistically distinguishable from controls (Table 5). Because these data were collected from the ~22% of surviving female gametes, we cannot, however, exclude the possibility that there may be selection that favors gametes with higher rates of meiotic crossovers. Even so, the significant number of chiasmata observed in male meiocytes (Table 3) provides additional evidence that meiotic crossovers occur in the *rad51* double mutant. Due to the complete sterility or lethality associated with *rad51* mutants, it has not been possible to measure rates of meiotic crossovers in Arabidopsis (Li *et al.* 2004) and vertebrates (Tsuzuki *et al.* 1996; Sonoda *et al.* 1998).

Does maize *dmc1* partially complement *rad51* in meiosis? This study demonstrates that in maize, as is true in yeast (Shinohara *et al.* 1992, 1997; Rockmill *et al.* 1995), *rad51* genes affect meiotic chromosome pairing, synapsis, and crossover, but are not essential.

We do not imply that the RAD51 protein is not involved in these processes. Rather, we hypothesize that in maize (unlike Arabidopsis) these roles of RAD51 can be at least partially complemented by other RecA homologs. If true, this maize homolog would be predicted to exhibit functional differences relative to the corresponding Arabidopsis homolog (Couteau *et al.* 1999; Bleuyard *et al.* 2005). Although there are multiple *rad51* paralogs in plants (Figure 1; Bleuyard *et al.* 2005), our working hypothesis, based on colocalization data from multiple species (Bishop 1994; Anderson *et al.* 1997; Tarsounas *et al.* 1999), *in vitro* functional analyses from humans and yeast (Sung 1994; Sehorn *et al.* 2004), and genetic data from yeast (Shinohara *et al.* 1997), is that one or both of the two maize *dmc1* genes (Franklin *et al.* 1999) can complement the meiotic chromosome pairing, synapsis, and crossover functions normally provided by RAD51, as has been proposed for yeast (Shinohara *et al.* 1997; Tsubouchi and Roeder 2003).

Absence of RAD51 leads to nonhomologous pairing and synapsis in meiosis: The maize *rad51* double mutant exhibits a phenotype that has not been observed in *rad51* mutants of other species. Specifically, we observed pairing, synapsis, and chiasmata between nonhomologous chromosomes. It has previously been demonstrated that nonhomologous synapsis occurs in mutants such as *phs1* (Pawlowski *et al.* 2004); the chiasmata observed between nonhomologous chromosomes in the *rad51* double mutant suggests that crossovers can occur between these nonhomologous chromosomes as occurs in the *ph* mutant of wheat (Riley and Chapman 1964; Riley *et al* 1966). In yeast, Rad51p has been shown to function in mediating strand exchange (Sung 1994; Benson *et al.* 1998; New *et al.* 1998; Shinohara and Ogawa 1998). It is possible that other RecA-like maize proteins, in the absence of RAD51, cannot efficiently mediate strand invasion and this inefficiency leads to nonhomologous pairing and synapsis in meiosis. On the other hand, the low percentage of nonhomologous pairing (Figure 9), nearly normal synapsis (Figure 10, A–C), and close to normal rates of meiotic crossovers from female surviving gametes (Table 5) suggest that other maize RecA homologs do an imperfect but adequate job to mediate strand invasion in *rad51* double mutants. These findings lead us to propose that in maize, RAD51 functions to increase, directly or indirectly, the precision of homologous pairing during meiosis.

We thank Pramod Mahajan (Pioneer Hi-Bred International) for stimulating discussions, Suling Zhao (Pioneer-Hi Bred International) for technical assistance with identifying TUSC alleles for *rad51* genes, Marianne Smith of the Schnable laboratory for technical assistance with light microcopy, and graduate student Sanzhen Liu for help with modifying figures. This research was supported by grants to P.S.S. from Pioneer Hi-Bred International and from the National Research Initiative of the USDA Cooperative State Research, Education and Extension Service, grant nos. 2001-35301-10685 and 2005-35301-15715. Additional support was provided by Hatch Act and State of Iowa funds.

LITERATURE CITED

Ananiev, E. V., R. L. Phillips and H. W. Rines, 1998 Chromosome-specific molecular organization of maize (*Zea mays* L.) centromeric regions. Proc. Natl. Acad. Sci. USA **95:** 13073–13078.

Anderson, L. K., H. H. Offenberg, W. M. Verkuijlen and C. Heyting, 1997 RecA-like proteins are components of early meiotic nodules in lily. Proc. Natl. Acad. Sci. USA **94:** 6868–6873.

Barkan, A., and R. A. Martienssen, 1991 Inactivation of maize transposon *Mu* suppresses a mutant phenotype by activating an outward-reading promoter near the end of *Mu1*. Proc. Natl. Acad. Sci. USA **88:** 3502–3506.

Bass, H. W., W. F. Marshall, J. W. Sedat, D. A. Agard and W. Z. Cande, 1997 Telomeres cluster de novo before the initiation of synapsis: a three-dimensional spatial analysis of telomere positions before and during meiotic prophase. J. Cell Biol. **137:** 5–18.

Bensen, R. J., G. S. Johal, V. C. Crane, J. T. Tossberg, P. S. Schnable *et al.*, 1995 Cloning and characterization of the maize *An1* gene. Plant Cell **7:** 75–84.

Benson, F. E., P. Baumann and S. C. West, 1998 Synergistic actions of Rad51 and Rad52 in recombination and DNA repair. Nature **391:** 401–404.

Bishop, D. K., 1994 RecA homologs Dmc1 and Rad51 interact to form multiple nuclear complexes prior to meiotic chromosome synapsis. Cell **79:** 1081–1092.

Bleuyard, J. Y., and C. I. White, 2004 The Arabidopsis homologue of Xrcc3 plays an essential role in meiosis. EMBO J. **23:** 439–449.

Bleuyard, J. Y., M. E. Gallego, F. Savigny and C. I. White, 2005 Differing requirements for the Arabidopsis Rad51 paralogs in meiosis and DNA repair. Plant J. **41:** 533–545.

Bleuyard, J. Y., M. E. Gallego and C. I. White, 2006 Recent advances in understanding of the DNA double-strand break repair machinery of plants. DNA Repair **5:** 1–12.

Brown, W. E., D. S. Robertson and J. L. Bennetzen, 1989 Molecular analysis of multiple *Muatotor*-derived alleles of the *Bronze* locus of maize. Genetics **122:** 439–445.

Couteau, F., F. Belzile, C. Horlow, O. Grandjean, D. Vezon *et al.*, 1999 Random chromosome segregation without meiotic arrest in both male and female meiocytes of a *dmc1* mutant of Arabidopsis. Plant Cell **11:** 1623–1634.

Cui, X., A. P. Hsia, F. Liu, D. A. Ashlock, R. P. Wise *et al.*, 2003 Alternative transcription initiation sites and polyadenylation sites are recruited during *Mu* suppression at the *rf2a* locus of maize. Genetics **163:** 685–698.

da Costa e Silva, O., R. Lorbiecke, P. Garg, L. Muller, M. Wassmann *et al.*, 2004 The *Etched1* gene of *Zea mays* (L.) encodes a zinc ribbon protein that belongs to the transcriptionally active chromosome (TAC) of plastids and is similar to the transcription factor TFIIS. Plant J. **38:** 923–939.

Das, L., and R. Martienssen, 1995 Site-selected transposon mutagenesis at the *hcf106* locus in maize. Plant Cell **7:** 287–294.

Dempsey, E., 1994 Traditional analysis of maize pachytene chromosomes, pp. 432–441 in *The Maize Handbook*, edited by M. Freeling and V. Walbot. Springer-Verlag, New York.

Dietrich, C. R., F. Cui, M. L. Packila, J. Li, D. A. Ashlock *et al.*, 2002 Maize Mu transposons are targeted to the 5′ untranslated region of the *gl8* gene and sequences flanking *Mu* target-site duplications exhibit nonrandom nucleotide composition throughout the genome. Genetics **160:** 697–716.

Doutriaux, M. P., F. Couteau, C. Bergounioux and C. White, 1998 Isolation and characterisation of the *RAD51* and *DMC1* homologs from *Arabidopsis thaliana*. Mol. Gen. Genet. **257:** 283–291.

Franklin, A. E., J. McElver, I. Sunjevaric, R. Rothstein, B. Bowen *et al.*, 1999 Three-dimensional microscopy of the Rad51 recombination protein during meiotic prophase. Plant Cell **11:** 809–824.

Gaut, B. S., M. Le Thierry d'Ennequin, A. S. Peek and M. C. Sawkins, 2000 Maize as a model for the evolution of plant nuclear genomes. Proc. Natl. Acad. Sci. USA **97:** 7008–7015.

Golubovskaya, I. N., L. C. Harper, W. P. Pawlowski, D. Schichnes and W. Z. Cande, 2002 The *pam1* gene is required for meiotic bouquet formation and efficient homologous synapsis in maize (*Zea mays* L.). Genetics **162:** 1979–1993.

Golubovskaya, I. N., O. Hamant, L. Timofejeva, C. R. Wang, D. Braun *et al.*, 2006 Alleles of *afd1* dissect REC8 functions during meiotic prophase I. J. Cell Sci. **119:** 3306–3315.

Goodman, M. M., C. W. Stuber, K. Newton and H. H. Weissinger, 1980 Linkage relationships of 19 enzymes loci in maize. Genetics **96:** 697–710.

Grishchuk, A. L., and J. Kohli, 2003 Five RecA-like proteins of *Schizosaccharomyces pombe* are involved in meiotic recombination. Genetics **165:** 1031–1043.

Hamant, O., H. Ma and W. Z. Cande, 2006 Genetics of meiotic prophase I in plants. Annu. Rev. Plant Biol. **57:** 267–302

Hays, S. L., A. A. Firmenich and P. Berg, 1995 Complex formation in yeast double-strand break repair: participation of Rad51, Rad52, Rad55, and Rad57 proteins. Proc. Natl. Acad. Sci. USA **92:** 6925–6929.

Higgins, J. D., E. Sanchez-Moran, S. J. Armstrong, G. H. Jones and F. C. Franklin, 2005 The Arabidopsis synaptonemal complex protein ZYP1 is required for chromosome synapsis and normal fidelity of crossing over. Genes Dev. **19:** 2488–2500.

Levy, A. A., and V. Walbot, 1991 Molecular analysis of the loss of somatic instability in the *bz2::mu1* allele of maize. Mol. Gen. Genet. **229:** 147–151.

Levy, A. A., A. B. Britt, K. R. Luehrsen, V. L. Chandler, C. Warren *et al.*, 1989 Developmental and genetic aspects of *Mutator* excision in maize. Dev. Genet. **10:** 520–531.

Li, W., C. Chen, U. Markmann-Mulisch, L. Timofejeva, E. Schmelzer *et al.*, 2004 The *Arabidopsis AtRAD51* gene is dispensable for vegetative development but required for meiosis. Proc. Natl. Acad. Sci. USA **101:** 10596–10601.

Li, W., X. Yang, Z. Lin, L. Timofejeva, R. Xiao *et al.*, 2005 The *AtRAD51C* gene is required for normal meiotic chromosome synapsis and double-stranded break repair in Arabidopsis. Plant Physiol. **138:** 965–976.

Martienssen, R., and A. Baron, 1994 Coordinate suppression of mutations caused by Robertson's *mutator* transposons in maize. Genetics **136:** 1157–1170.

McClintock, B., 1934 The relation of a particular chromosomal element to the development of the nucleoli in *Zea mays*. Z. Zellforsch. Mikroskop. Anat. **21:** 294–328.

Nara, T., T. Yamamoto and K. Sakaguchi, 2000 Characterization of interaction of C- and N-terminal domains in *LIM15/DMC1* and *RAD51* from a basidiomycetes, *Coprinus cinereus*. Biochem. Biophys. Res. Commun. **275:** 97–102.

New, J. H., T. Sugiyama, E. Zaitseva and S. C. Kowalczykowski, 1998 Rad52 protein stimulates DNA strand exchange by Rad51 and replication protein A. Nature **391:** 407–410.

Ogawa, T., X. Yu, A. Shinohara and E. H. Egelman, 1993 Similarity of the yeast RAD51 filament to the bacterial RecA filament. Science **259:** 1896–1899.

Pawlowski, W. P., I. N. Golubovskaya and W. Z. Cande, 2003 Altered nuclear distribution of recombination protein RAD51 in maize mutants suggests the involvement of RAD51 in meiotic homology recognition. Plant Cell **15:** 1807–1816.

Pawlowski, W. P., I. N. Golubovskaya, L. Timofejeva, R. B. Meeley, W. F. Sheridan *et al.*, 2004 Coordination of meiotic recombination, pairing, and synapsis by PHS1. Science **303:** 89–92.

Riley, R., and V. Chapman, 1964 Cytological determination of the homoeology of chromosomes of *Triticum aestivum*. Nature **203:** 156–158.

Riley, R., V. Chapman, R. M. Young and A. M. Belfield, 1966 Control of meiotic chromosome pairing by the chromosomes of homoeologous group 5 of *Triticum aestivum*. Nature **212:** 1475–1477.

Robertson, D. S., 1978 Characterization of a mutator system in maize. Mutat. Res. **51:** 21–28.

Robertson, D. S., 1980 The timing of *Mu* activity in maize. Genetics **94:** 969–978.

Robertson, D. S., 1981 Mutator activity in maize: timing of its activation in ontogeny. Science **213:** 1515–1517.

Roca, A. I., and M. M. Cox, 1990 The RecA protein: structure and function. Crit. Rev. Biochem. Mol. Biol. **25:** 415–456.

Rockmill, B., M. Sym, H. Scherthan and G. S. Roeder, 1995 Roles for two RecA homologs in promoting meiotic chromosome synapsis. Genes Dev. **9:** 2684–2695.

Schnable, P. S., P. A. Peterson and H. Saedler, 1989 The *bz-rcy* allele of the *Cy* transposable element system of *Zea mays* contains a *Mu*-like element insertion. Mol. Gen. Genet. **217:** 459–463.

Sehorn, M. G., S. Sigurdsson, W. Bussen, V. M. Unger and P. Sung, 2004 Human meiotic recombinase Dmc1 promotes ATP-dependent homologous DNA strand exchange. Nature **429:** 433–437.

Shinohara, A., and T. Ogawa, 1998 Stimulation by Rad52 of yeast Rad51-mediated recombination. Nature **391:** 404–407.

Shinohara, A., H. Ogawa and T. Ogawa, 1992 Rad51 protein involved in repair and recombination in *S. cerevisiae* is a RecA-like protein. Cell **69:** 457–470.

Shinohara, A., S. Gasior, T. Ogawa, N. Kleckner and D. K. Bishop, 1997 *Saccharomyces cerevisiae* recA homologues RAD51 and DMC1 have both distinct and overlapping roles in meiotic recombination. Genes Cells **2:** 615–629.

Sonoda, E., M. S. Sasaki, J. M. Buerstedde, O. Bezzubova, A. Shinohara *et al.*, 1998 Rad51-deficient vertebrate cells accumulate chromosomal breaks prior to cell death. EMBO J. **17:** 598–608.

Sung, P., 1994 Catalysis of ATP-dependent homologous DNA pairing and strand exchange by yeast RAD51 protein. Science **265:** 1241–1243.

Tarsounas, M., T. Morita, R. E. Pearlman and P. B. Moens, 1999 RAD51 and DMC1 form mixed complexes associated with mouse meiotic chromosome cores and synaptonemal complexes. J. Cell Biol. **147:** 207–220.

Taylor, L. P., and V. Walbot, 1985 A deletion adjacent to the maize transposable element Mu-1 accompanies loss of Adh1 expression. EMBO J. **4:** 869–876.

Terasawa, M., A. Shinohara, Y. Hotta, H. Ogawa and T. Ogawa, 1995 Localization of RecA-like recombination proteins on chromosomes of the lily at various meiotic stages. Genes Dev. **9:** 925–934.

Tsubouchi, H., and G. S. Roeder, 2003 The importance of genetic recombination for fidelity of chromosome pairing in meiosis. Dev. Cell **5:** 915–925.

Tsuzuki, T., Y. Fujii, K. Sakumi, Y. Tominaga, K. Nakao *et al.*, 1996 Targeted disruption of the Rad51 gene leads to lethality in embryonic mice. Proc. Natl. Acad. Sci. USA **93:** 6236–6240.

Zimmer, E. A., E. R. Jupe and V. Walbot, 1988 Ribosomal gene structure, variation and inheritance in maize and its ancestors. Genetics **120:** 1125–1136.

Communicating editor: T. P. Brutnell